Chandrashekhar et al., J Material Sci Eng 2016, 5:4
DOI: 10.4172/2169-0022.1000251

Journal of Material Science & Engineering

Research Article Open Access

Scratch Wear Resistance of TiALN And AlCrN Coated EN-353 Steel

Chandrashekhar A[1]*, Kabadi VR[2] and Bhide R[3]

[1]Department of Mechanical Engineering, Basaveshwar Engineering College, Bagalkot, India
[2]Department of Mechanical Engineering, Nitte Meenakshi Institute of Technology, Bangaluru, India
[3]Application Support Centre, Oerlikon Balzers Coating India Limited, Bhosari, Pune, Maharashtra, India

Abstract

TiAlN and AlCrN coatings were deposited on mild steel (EN 353 steel) by cathodic arc evaporation technique. Coefficients of friction, critical load, adhesive and cohesive properties of these coatings were studied using scratch tester. Failure mode for coatings with thickness of 2 and 4 μm were studied using scratch channels and acoustic activities as basis. Studies presented relationship between progressive and in situ emission signals. AlCrN coating exhibited higher critical load as determined by the acoustic emission signal. Additionally wear mechanisms were analyzed. Analysis of the experimental results showed that load carrying capacity of AlCrN coating is better than TiAlN coating. Scratch wear test of AlCrN coated substrates showed reduction in cracking and spalling of coated layers.

Keywords: TiAlN and AlCrN coatings; Magnetron sputtering; Scratch testing; Scratch resistance

Introduction

For variety of applications, improved tribological properties has become an important aspect in the development of high performance materials [1]. In this direction, coatings are widely used to reduce the coefficient of friction as well as wear loss in all types of sliding contacts. Much excellent information on coated components in automobile applications has been achieved. Majority of sliding components have shown reduction in the coefficient of friction by two orders of magnitude. For example, by coating a steel substrate with molybdenum disulphide or diamond, this slides against a steel counterface, the wear loss has been reduced several orders of magnitudes compared with the uncoated pairs in contact [2].

Thermal spraying, electro deposition, chemical vapour deposition (CVD), and physical vapour deposition (PVD) etc. are some of the coating methods commercialized recently [3-5]. Improvement in hardness, lower friction and corrosion resistance of surfaces in tool like drilling etc., is achieved by coating them with TiN, CrN, TiAlN, AlTiN, TiCN, WC, AlCrN, multi layers of TiN and TiAlN [6]. The tribological properties of steels are generally improved with deposition of PVD coatings; the durability of the coating depends not only on the properties of coating but also on the adhesion of the coating and the substrate as reported by Totik [7]. High hardness, low coefficient of friction, high wear resistance and good oxidation resistance makes titanium nitride (TiN) an industrially popular coating. These properties make this an ideal candidate material for various tribological applications. TiN coatings have been most commonly used in the applications of forging tools, molds, cutting tools, bearing spindles and many mechanical components to decorative items because of its resistance to wear, corrosion and temperature [8-12]. The tribological behaviour of TiN, AlTiN and AlCrN films were investigated that vary with substrate roughness, thickness of the film coating, hardness of the substrate, deposition method, type of wear, stoichiometry and type of heat treatment. For hard substrates are relatively brittle like ceramics, the hard coating materials are TiN, AlTiN and AlCrN films. They have a great tendency to fracture and spall from the substrate during wear. Such tendency increases with increasing the applied load, sliding speed and coating thickness [13]. In recent years, studies on aluminium titanium nitride (AlTiN) and aluminium chromium nitride (AlCrN) coatings have been increased [14-16].

In most of the mechanical industries, EN-353 low carbon steel is widely used because of its good ductility and weldability. This material has poor tribological properties such as high coefficient of friction, low wear resistance, and low hardness [17]. Two methods are commonly used to improve the tribological behaviour of steel. Firstly, adding alloy elements to the steel during smelting of the integral alloy and secondly, by surface modification. The former is impractical because number of interstitial elements doped into the steel is harmful to ductility and increase the cost of products. Thus, surface modification is an effective and economical method that has become one of the most popular research fields in recent years. A wide variety of surface modifications of steels are viable routes to improve tribological properties viz., PVD and ion plating. An advantage of the technology is that the coatings are metallurgically bonded to the substrate with good interface. It also exhibits a high deposition rate, good coating uniformity, and controllability of coating thickness to complex shaped substrates.

The scratch test is one of the most convenient methods to use and no special dimension specimen or preparation is required compared to other methods. Therefore, to investigate the adhesion of thin coating-substrate scratch tester has increasingly been used [18]. Adhesion strength of thin films is measured using ramp progressive load scratch tester where in a normal load applied to the coating surface is increased and the load, at which coating fails adhesively, is taken as the critical load for coating failure. This test can be used to determine the wear behaviour of a material under different stresses. The strength of adhesion is influenced by many factors: the substrate hardness, the coating thickness, the surface quality, the coating hardness, the loading rate, interface bonding, indenter dimensions, and the friction between the indenter and a coating [19].

Although a great deal of research work has been carried out on friction and wear behaviour of various coatings, very limited work has

***Corresponding author:** Chandrashekhar A, Department of Mechanical Engineering, Basaveshwar Engineering College, Bagalkot, India, Tel: 8333278887; Fax: 8333278886; E-mail: chandrashekhar_dev@yahoo.co.in

Received April 04, 2016; **Accepted** May 10, 2016; **Published** May 20, 2016

Citation: Chandrashekhar A, Kabadi VR, Bhide R (2016) Scratch Wear Resistance of TiALN And AlCrN Coated EN-353 Steel. J Material Sci Eng 5: 251. doi:10.4172/2169-0022.1000251

been done on scratch behaviour of TiAlN and AlCrN coatings. Against this background, the present work, we have studied the relation between the wear resistance and the scratch behaviour for comparing different hard coatings with different soft and hard substrates. The critical load values depend upon the hardness of the substrate, when scratching a specimen with a thin coating. Increasing the thickness of coating the critical load values causes to rise.

Materials and Methods

Materials

The EN-353 steel substrate of the actual chemical composition were analysed with the help of Optical Emission spectrometer (Thermo Electron S. A. En Vallaire Quest 1024, Ecublens, Switzerland make). The nominal and actual chemical composition of the substrates used in the present investigation are listed in Table 1.

Deposition method

The substrate used was mild steel (EN 353 steel), consisting of 0.217% C. The substrate surface was ground with SiC paper to remove the oxides and other contamination. Prior to deposition, substrates were initially degreased in ultrasonic bath to remove excessive oils and greases. This is followed by cleaning with alkaline solutions and rinsing with Demineralized Water (DM). Final stage of cleaning includes drying with hot air blower. Cleaning of these parts was carried out using Oerlikon Balzers proprietary (standard) cleaning procedure.

TiAlN and AlCrN coatings were carried out with arc evaporation method using Oerlikon Blazers commercial coating process. Customized TiAl and AlCr target in reactive nitrogen atmosphere were used to obtain stoichiometric TiAlN and AlCrN coating. The thicknesses of the AlCrN coatings were approximately 2 ± 0.3 and 4 ± 0.2 µm. Coating was carried out at temperature of about 500 ± 10°C with nitrogen as reactive gas. A DC-substrate bias voltage was maintained in the range of -50 to -150V during coating.

Microstructure

A Zeiss Axiovert 200 MAT inverted optical microscope, fitted with image software Zeiss Axiovision Release 4.1, was used for optical microscopy. The porosity measurements were made with image analyser, having software of Dewinter Materials Plus 1.01 based on ASTM B276. A PMP3 inverted metallurgical microscope was used to obtain the images.

Hardness

Hardness measurements for the compound system of substrate + coating were carried out as per the IS 1501-2002 procedures by using Vickers hardness tester (MH6). The hardness of the coatings on steel was measured using a VH-1 (METATECH) hardness tester, applying a load of 10, 25 and 50 g and a dwell time of 15 seconds. To measure the hardness of the coating a nano-indenter was used. The hardness was measured in three different locations and the readings reported are the average of the three readings.

X-ray diffraction

The coated specimens were subjected to XRD pattern was recorded using computer controlled XRD-system, JEOL, and Model: JPX-8030 with CuK radiation. The scan rate used was 2°/min and the scan range was from 10° to 120°. The grain size of the thin films was estimated from Scherrer formula, as given in Eq. (1). In this expression, the grain size D is along the surface normal direction, which is also the direction of the XRD diffraction vector.

$$D = \frac{0.9\tau}{B\cos\theta} \quad (1)$$

where B is the corrected full-width at half maximum (FWHM) of a Bragg peak, λ is the X-ray wavelength, and θ is the Bragg angle. B is obtained from the equation $B^2=B^2_r-B^2_{strain}-C^2$, where B_r is the FWHM of a measured Bragg peak, $B_{strain} = \varepsilon \tan\theta$ is the lattice broadening from the residual strain ε measured by XRD using the $\cos^2\alpha \sin^2\psi$ method, and C is the instrumental line broadening.

Surface roughness

The surface morphology (2D and 3D) of the thin films was characterized by atomic force microscopy (AFM) to calculate the surface roughness and particle size. Innova SPM atomic force microscope works in both contact and tapping mode. Contact Mode is the most straightforward, basic topography imaging mode of the AFM. In contact mode, the AFM tip has a direct contact with the sample. While the tip is scanned along the surface, the sample topography induces a vertical deflection of the cantilever. This deflection is measured by a fiber- optical interferometer. On the other hand, the tapping mode maps topography by lightly tapping the surface with an oscillating probe tip. The cantilever's oscillation amplitude changes with sample surface topography, and the topography image is obtained by monitoring these changes and closing the z feedback loop to minimize them. It overcomes some of the limitations of both contact and non-contact AFM.

Scratch testing

Wear behaviour tests were carried out on the DUCOM scratch tester TR101 (Figure 1) under dry conditions, in ambient air at room temperature (≈ 25°C). Micro scratch tester have a Rockwell shaped C spherical indenter with a normal radius of 200 µm and an angle of 120° was used. A schematic diagram of scratch tester is presented in Figure 2. The sample for scratch test experiments substrates were machined with dimensions of 60 mm × 25 mm × 10 mm.

The indenter velocity was used over a wear tracks of 14 mm, with different normal loads applied. PLST (Progressive Loading

Figure 1: Photograph of scratch tester TR-101.

Elements	C	Mn	Si	P	S	Ni	Cr	Mo	Fe
Nominal	0.1-0.2	0.5-1.0	0.35	0.05	0.05	1-1.5	0.75-1.25	0.08-0.15	Bal.
Actual	0.217	0.57762	0.1895	0.0582	0.0487	0.0317	0.05306	0.00459	Bal.

Table 1: Chemical composition by wt % of EN-353 steel.

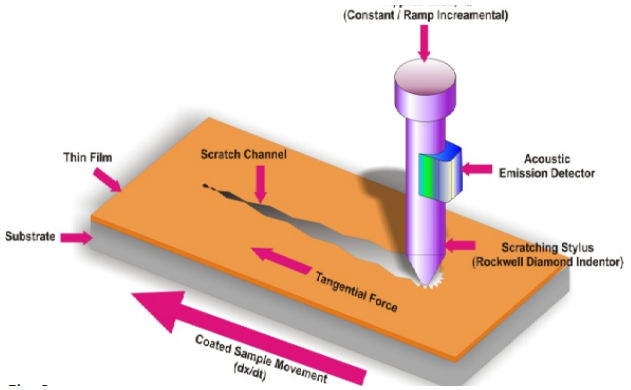

Figure 2: Schematic diagram of scratch tester.

Scratch Test) mode of scratch testing was used. In PLST mode the normal load was increased linearly during the test from 10 to 160 N. The indenter scratches the coated substrate linearly with increasing load progressively. Scratch adhesion testing is loaded stylus drawn a spherically tipped diamond indenter over the surface of a coated sample under a normal force increasing vertical load either stepwise or continuously until coating becomes seperates completely from the scratch channel. The value of the critical load is considered as of the coating–substrate adhesion [20,21]. The critical loads for full delamination were determined from the recorded normal force, tractional force, coefficient of friction and acoustic emission along the scracth; the respective images have also been taken.

Worn surface morphology

Scanning electron microscope (SEM-JEOL, Model-JSM 6380) is used to study the behavioral surface morphology of the coatings. SEM micrographs were taken with electron beam energy of 15 keV.

Results and Discussion

Coating microstructures

The TiAlN and AlCrN coatings have been formulated successfully by PVD (physical vapour deposition) technique on EN-353 steel. The optical micrographs of the substrate, TiAlN and AlCrN coatings indicating dense, fine grained columnar structures and are depicted in Figures 3 and 4. Figures 3a and 3b shows the microstructure of TiAlN coating is violet-grey in color and blue-grey in case of AlCrN (Figures 4a and 4b) coating. The coatings have uniform microstructure. It is evident from the microstructure that the coatings contain some pores and inclusions. The porosity for as-coated TiAlN and AlCrN coatings is 0.47% and 0.46% respectively [22].

Vicker's microhardness

Hardness values for coatings with TiAlN and AlCrN films with 2 and 4 μm thickness on EN-353 steel are summarised in Table 2. The Vicker microhardness of TiAlN and AlCrN coatings were around Hv`= 1081 to 1216, and increased with increase in coating thickness. As expected from theretical considerations, the coating hardness increased with target hardness, and film thickness, and decreased with

Samples (thickness)	50 g	25 g	10 g
AlCrN (2 μm)	634	1034	1094
AlCrN (4 μm)	718	1102	1216
TiAlN (2 μm)	622	1027	1081
TiAlN (4 μm)	689	1083	1197

Table 2: Vicker's hardness of AlCrN and TiAlN coatings on MS at different loads.

increasing indentation load. The increase in hardness was observed with the decrease in load as listed in Table 2. With the incorporation of AlCrN film of ~2 μm to ~4 μm thick, the microhardness increases from 1094 to 1216 at 10 g load. However, the TiAlN coating Vickers micro-hardness was lower than that of AlCrN coating, which is about Hv = 1081 to 1197, may be because of the pores in the coatings.

The difference in the micro-hardness is in coincidence with the variation of the coating structure especially the density and porosity of the coating. Further, the influence of thickness of the AlCrN coating on the Vicker's micro-hardness was related to the coating structure (Figure 3a and 3b). Inside the thick coating (4 μm) AlCrN coating (Figure 3b) the densed AlCrN film was formed.

Crystal structure of AlCrN and TiAlN coatings

XRD spectra for AlCrN and TiAlN coating thickness of 2 and 4 μm are depicted in Figures 5 and 6 on reduced scale. XRD analysis for AlCrN coating confirmed the presence of CrN and AlN phases. Further, in case of TiAlN coating the prominent phases are a large percentage of Ti_2N along with AlN. From the XRD spectra, the grain size of the thin coatings was estimated from Scherrer formula as given in Eq. (1), and reported in Table 3. The grain size in case of TiAlN coatings (15 nm) is less than that of AlCrN coating (21 nm). Sample TiAlN coating with thickness 2 μm showed a strong preferred lattice (ε) planes have a dominant orientation at 44.92° (2θ), as shown in Figure 5. The preferred lattice plane is caused by the mobility of atoms which decreases with increasing Al/Ti ratio. In contrast, in the case of the AlCrN coating, the lattice planes (α) have a dominant orientation at 49.637° (2θ), as shown in Figure 6. The intensities of the diffraction peaks gradually decrease with increasing layer thickness, which indicates a gradual decrease in grain size of the preferred orientation. Oerlikon Balzers Ltd. India provided the data regarding hardness and the friction coefficient against steel (dry), along with the coating parameters (Table 3). The coated layer on the steel substrate has provided higher hardness as compared to the substrate. TiAlN coating showed higher hardness value than AlCrN coating as reported in Table 2.

Effect of surface roughness

Surface roughness either from the substrate or coating influences the scratch test data. Hence surface roughness of the coated surfaces prior to testing is essential. Surface roughness also influences the friction as well as wear performance of a mechanical system like sleeves used in bearings. It has also been shown from the literature on hard coatings that the rougher the surface finish, the lower will be the coating adhesion and wear resistance [1]. All morphologies exhibited domes and craters which are uniformly distributed over the entire surface. Figure 7 shows the roughness values of the TiAlN and AlCrN coated on EN-353 steel containing film thickness of 2 and 4 μm. The roughness of the TiAlN coated substrate is nearly two times higher

Coating Type	Coating thickness(μm)	Arithmetic mean roughness Ra (nm)	Maximum height Rq (nm)	Point mean roughness Rmax(nm)	Appearance of surface features
AlCrN	~ 2	235	297	2779	Irregularly spaced peaked features
TiAlN	~ 2	244	306	2340	Irregularly spaced peaked features
AlCrN	~ 4	165	206	1702	Irregularly spaced peaked features
TiAlN	~ 4	221	274	2224	Irregularly spaced peaked features

Table 3: Results demonstrated variation in the size and height of surface nano-topographs of TiAlN and AlCrN coatings.

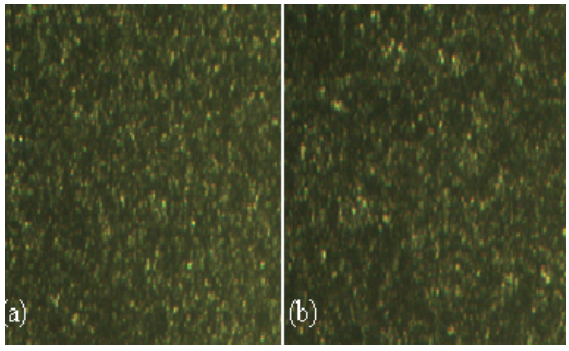

Figure 3: Optical micrographs of the coated surface of (a) AlCrN with 2 μm coating, (b) AlCrN with 4 μm coating.

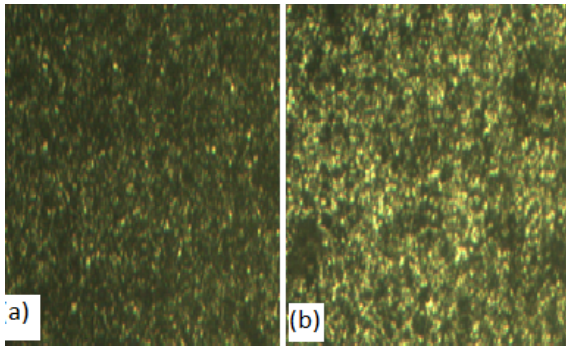

Figure 4: Optical micrographs of the coated surface of (a) TiAlN with 2 μm coating, and (b) TiAlN with 4 μm coating.

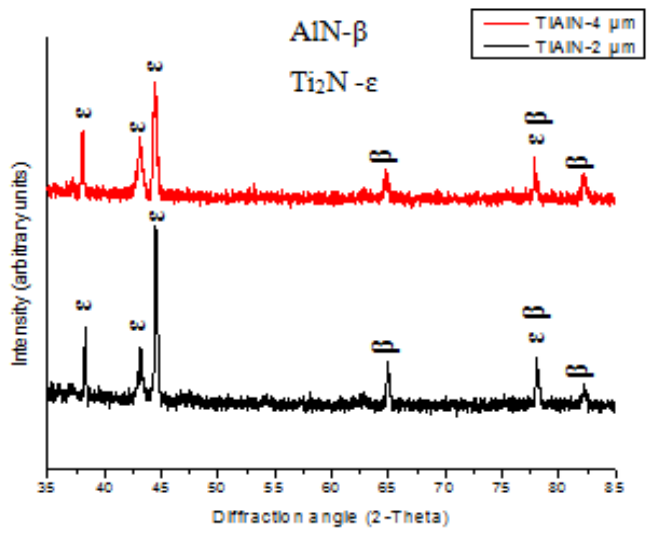

Figure 5: X-ray diffraction pattern for ~2 & ~4 μm TiAlN coating on mild steel substrate (EN-353).

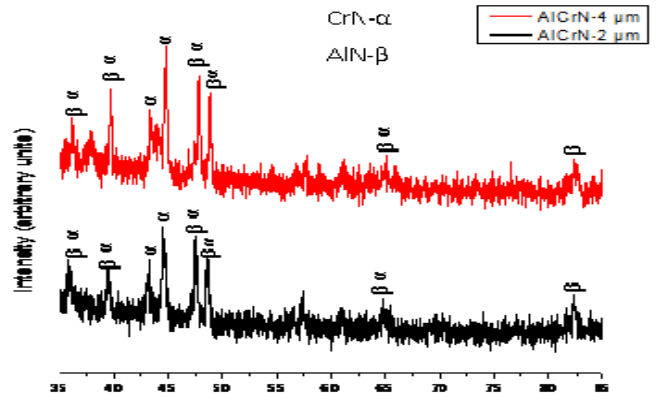

Figure 6: X-ray diffraction pattern for ~2 & ~4 μm AlCrN coating on mild steel substrate (EN-353).

than that of the AlCrN coated substrate. The Ra values are low at 2 μm coating thickness and increases with increasing coating thickness. Higher roughness values especially in 4 μm indicate the presence of little agglomeration. A higher roughness value leads to easy pull-out of coated film in wear scratch testing. Figure 7 shows the typical roughness profile of the TiAlN and AlCrN coated on EN 353 steel substrates with a Ra value of 1.2 μm and 0.93 μm respectively. The roughness profiles of TiAlN and AlCrN coated on EN 353 steel substrates are similar to the literature findings [23,24].

Figures 7a-7d shows the difference in morphology between the two films can be inferred by comparing the 2D images in Figures 7a and 7b; however, a clearer comparison of the films is afforded by viewing the 3D images in Figures 7c and 7d. Surface roughness of all the coatings increases after deposition. By increasing the coating thickness, the surface roughness turns to smoother and smoother as shown in Table 3. i.e., the area distributed with protrusions becomes larger as the coating films become thicker. The surface morphology explained that coating surface roughness results from the sharps of nucleus, from preferential nucleation at substrate inhomogeneties, from the coating thickness and preferential growth. The fluctuation of coating thickness results in the surface energy fluctuation. The 2 and 4 μm AlCrN coatings are found to give very finest asperities compared to TiAlN coatings, i.e., the morphology induced by the coating growth process and morphology of the coating thickness. The increase in coating thickness results in the fine-grained morphology of the coating surface with decreased the asperities. A surface with a higher value of Ra or Rq implies less uniformity.

Scratch resistance

Adhesion of a coating is one of the important properties for better load carrying capacity and scratch resistance of a coating system. If a coating does not adhere to the substrate, burning, cracking or peeling off the deposit would occur affecting the performance of the coating. The damage can be a cracking of the coating at the interface;

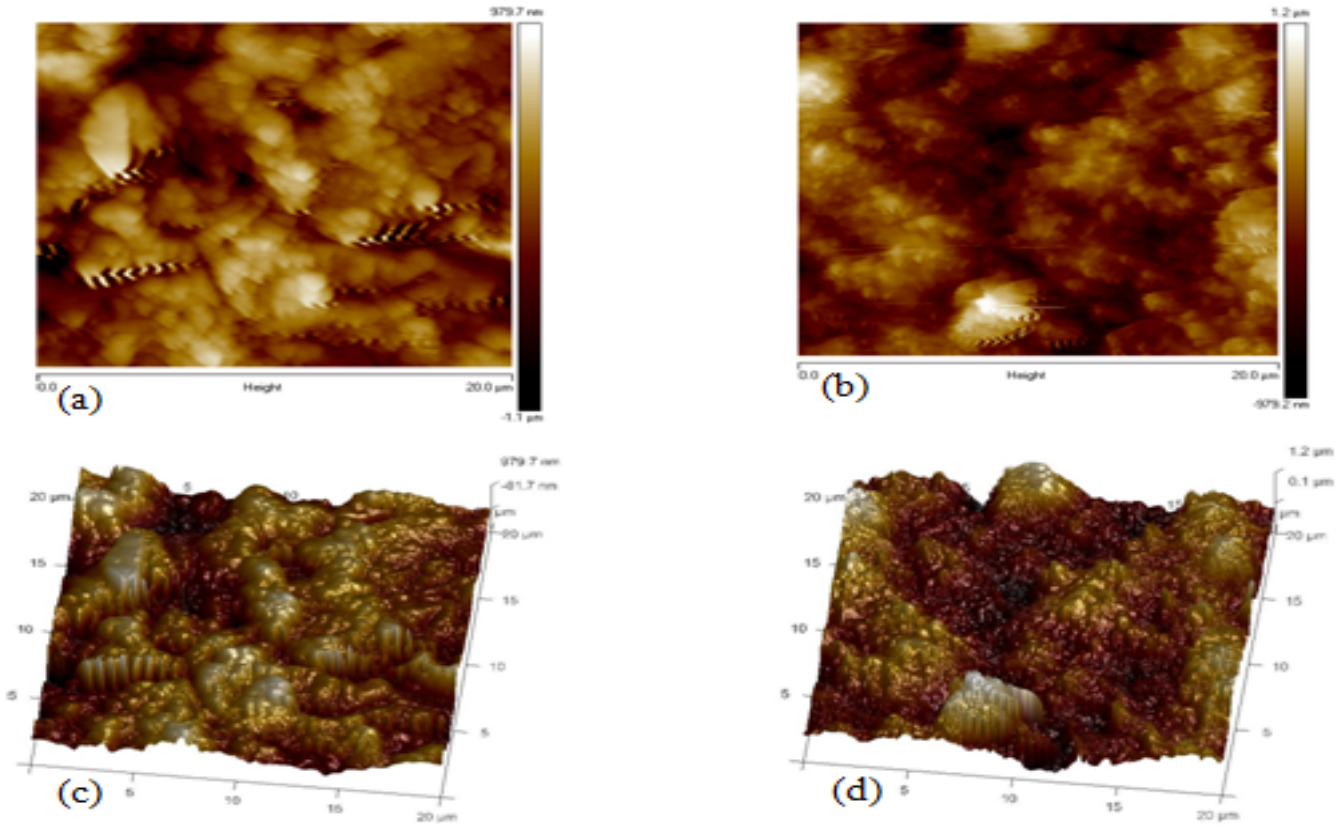

Figure 7: 2D and 3D AFM images of coatings: (a) AlCrN [(a) & (c) and TiAlN [(b) & (d)] 2 µm coatings deposited on EN-353 steel.

this indicates an adhesive type of failure. If the damage consists of chipping within the coating itself, then it is called a cohesive type of failure. The scratch test has achieved the most widespread use in assessing the adhesive strength of hard coated substrates of all the tests available for the measurement of coating adhesion. The test consists of applying an incrementally or continuously increasing load on the system at constant speed. The scratching point causes increasing elastic and plastic deformation until damage occurs in the surface region. In practice, the film is seldom removed entirely from the channel so it is convenient to define a critical load, which characterizes the mechanical adhesive strength of the coating-substrate system [25-30].

Scratch test shows variation of traction force (tangential force) and normal load (applied load) from start point to end point of the scratch. In this test, with the applied force, the traction force suddenly shows a peak and then attains a steady state value. The failure of the coating, whether cohesive/adhesive, is normally indicated by a pointed rise in the traction force. The lower value (base of the peak) of this traction force corresponds to the first sign of coating failure while the upper end (top of the peak) corresponds to the end of the failure. Scratch resistance is the normal load applied on the stylus corresponding to the above two values in traction force. It is minimum normal load required to delaminate coating from its substrate. However, due to the fact that there is a distribution of flaws at the coating substrate interface, isolated areas of coating removal do occur and the critical transitions can be somewhat subjective [31].

Number of experiments was carried out on two types of coated systems on EN-353 steel as substrate. The scratches on the coated substrates were linear progressively increasing load. Variation of the different characterizations obtained for three different sliding speeds are 0.1, 0.5 and 1.0 mm/s along with different start loads and loading rates are 10, 20 and 40 N and 2, 5 and 10 N/mm respectively are presented in Figures 8 and 9.

The critical load values of the composite TiAlN and AlCrN films, which were deposited on the EN-353 steel with 2 different coating thickness are showing relationship between normal load, coefficient of friction and scratch distance are given in Figures 8 and 9. The progressive incremental load, as shown Figure 8a was applied over the coated samples through the diamond stylus. It is observed that with increase in the scratch length the normal load is increased with respective to the sliding speed. i.e., normal load is directly proportional to the scratch distance. Initially the indenter will penetrate in the coating material. With the increase in the penetration of the indenter in the coating material the normal load increases. The scratch test is in nothing but the single point cutting tool process like shaper. As the progressive load increases, the penetration of the indenter in the substrate increases. At beginning the indenter penetrate in the coating then to the substrate ahead of the indenter goes on collecting ahead of the indenter in the form of chip. At the lower normal load of about 14 N with variation of coefficient of friction, which initiates the propagation of the microcracks and adhesive failure shows that film has begun to remove from the substrate. A strong distortion of the variation of the traction force and the coefficient of friction was observed at a higher normal load indicating that the total removal of the coating from the substrate.

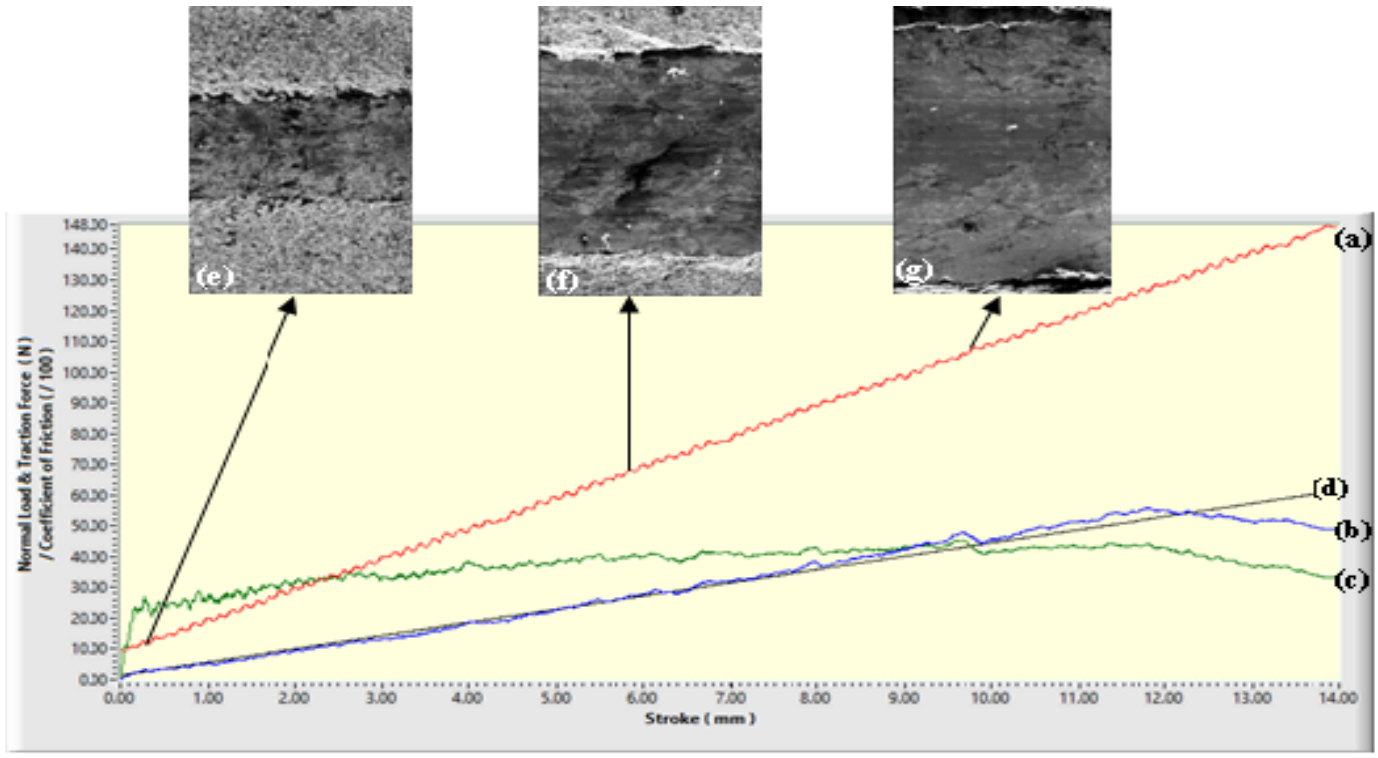

Figure 8: The typical images of scratch track along with graphs on the 2 µm TiAlN coated EN-353steel substrate at different locations. (Start Load- 10 N, Loading Rate- 10 N/mm, Scratch speed- 1.0 mm/sec and Scratch Stroke- 14 mm). a) Normal load, b) Tractional Force, c)Co-efficient of friction, d)Acoustic Emission, e)SEM, showing coating cracks at beginning, f) SEM, worn surface at middle, g) SEM, highly worn surface).

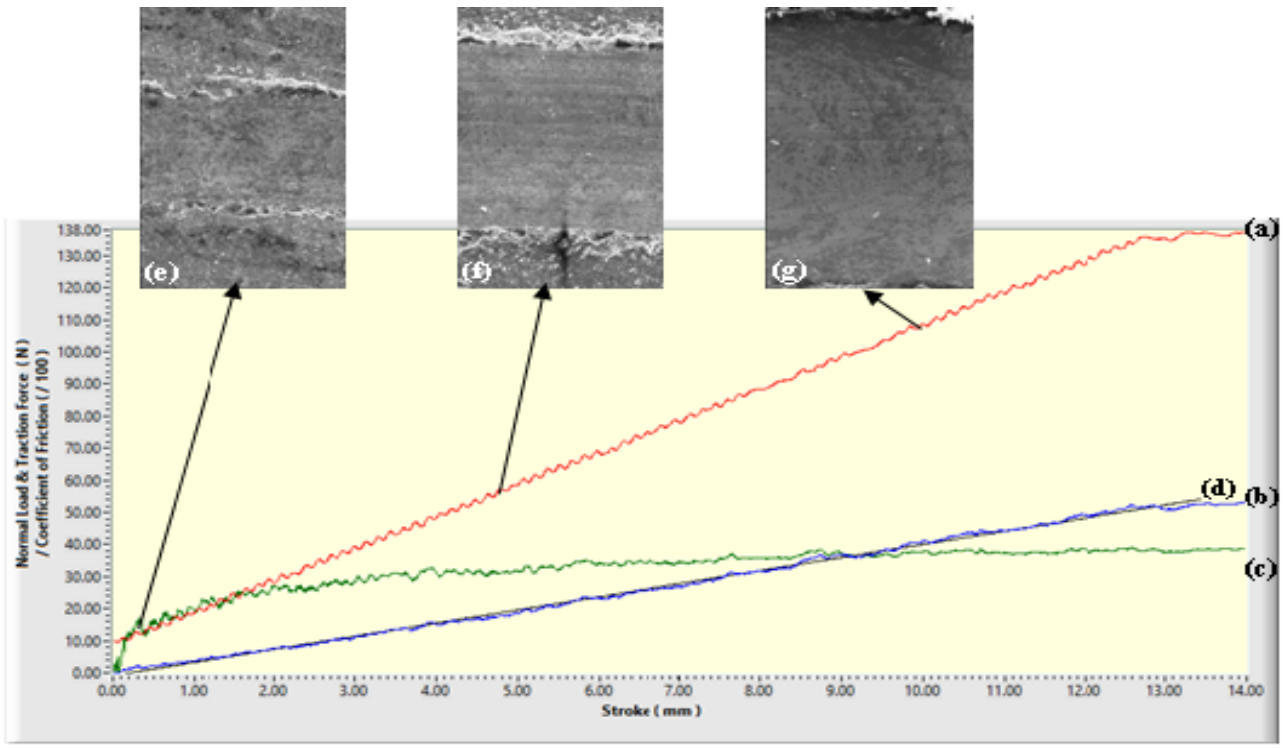

Figure 9: The typical images of scratch track along with graphs on the 2 µm TiAlN coated EN-353steel substrate at different locations. (Start Load- 10 N, Loading Rate- 10 N/mm, Scratch speed- 1.0 mm/sec and Scratch Stroke- 14 mm). a) Normal load, b) Tractional Force, c) Co-efficient of friction, d)Acoustic Emission, e) SEM, showing coating cracks at beginning, f) SEM, worn surface at middle, g) SEM, highly worn surface).

In Figure 8b indicates the variation of tractional force along scratch length on the TiAlN coating during scratch test. The traction force increased linearly with the increase in normal load and the slope changes indicates that the failure of coating material. It can see that the maximum tractional force 56 N takes place at scratch length 11.8 mm in the end part of the scratch, where the maximum depth of cut occurs [32]. Once the indenter crosses the thickness of the coating then the indenter penetrates inside the substrate material. Substrate material is softer than the coated material. Hence with further increase in the scratch length at 11.8 mm tractional force start decreases with increasing of the normal load. which may be due to the rate of collection of coating material ahead of the indenter is more when tractional force reaches a yield shear strength. This indicates that the total delamination of the coating from the substrate.

Figure 8c exhibits the coefficient of friction versus scratch distance curve, this can offer crucial clue to the determination of transition point in scratch damage mechanisms. The coefficient of friction is defined as tractional force and normal load. It is interesting to note that a changes of coefficient of friction (COF) slope that are obviously scratch damage feature, i.e., delamination, as scratch progresses. It was also observed that the fluctuation shown in COF curve, where tractional force increases gradually due to the penetration of the scratch tip into the substrate [33]. As seen from Figure 7 the COF increases initially around 0.3 mm scratch length and then remain nearly constant. The initial increase of the friction was considered to contain both adhesive and plouging friction [34]. Figure 8d shows the acoustic emission versus the scratch sliding stroke. The significance of scratch test carried out was that a direct correlation was detected about changes in the tractional force and coefficient of friction.

From Figure 9b it shows that higher tractional force were obtained for AlCrN coating than for TiAlN coating, which may be due to its higher plastic deformation resistance. Figure 9c shows lower coefficient of friction observed in AlCrN value of 0.38 as compared to the TiAlN coating which is 0.45. This confirms that the AlCrN coating has better wear resistance behaviour [5].

Graphical display of forces with almost linear increase in the traction force indicating scratch failure is of adhesive type for TiAlN and AlCrN coated EN 353 steel substrates which are shown in Figures 7 and 8, respectively. The Figure 7 also shows the traction loads corresponding to the normal loads representing the scratch failure. The AlCrN coated steel substrate shows that the failure, as indicated by the change in slope of the traction force, occurs at 110 N normal load, whereas it occurs at 90 N for the TiAlN coated steel substrate. It is also observed that the coefficient of friction of the AlCrN coated steel substrate is around 0.22 and 0.35 TiAlN coated steel substrate.

As it can be seen from the Figures 8 and 9, the frictional behaviour differs with varying sliding speed, start load and loading rate with the presence or absence of the protective layers like TiAlN and AlCrN coatings. Generally a rapid increase of the friction coefficient, reaching the local maximum value at the lowest speed, of 0.1 mm/s was detected at the primary 14 mm scratch stroke, independently of the scratch tested. Further, intermediate and higher speeds of sliding results in decreases the friction, which reaches the local minimum value promptly at a lower operational condition. Further tribological behaviour of the scratch tested depends significantly on the coating composition. AlCrN coating showed a slow increase of the coefficient of friction as compared to TiAlN coating.

For all the test coated substrates, the coefficient of friction, tangential force, normal load and acoustic emission with scratch length for all scratch tests, as shown coincide exact position with the typical topographically changes of the coatings by using and scanning electronic microscope along with the scratch track graphs.

Microscopic observations

On the basis of our experiments, we have adopted the approach whereby the adhesive wear loss is considered to be typical and significant when it occurs regularly along the scratch length (Figures 10 and 11). The coating can also be lost by cohesive failure of the substrate or by cohesive failure of the coating. These are both failures of the coating-substrate composite by a mechanism other than simple adhesive failure but both would correspond nevertheless to the failure of a part in service [35]. The scanning electron microscopy (SEM) examples shown in Figures 9e-9g was thought to be adhesive as well as cohesive failure in a TiAlN coated steel, whereas in Figures 10e-10g could be adhesive loss (flaking) in AlCrN coated steel substrate.

Scanning electron microscopy investigations of the scratched coated substrates were carried out in order to determine the mechanisms of material removal of the different coatings on substrates. SEM micrographs of the TiAlN coated EN353 steel are shown in Figures 10 and 11. During each experimental test, the normal load was increased from given start load until severe coating failure occurred (Figures 8 and 9). In most of the experiments, the critical normal load, Pc, at which coating failure initiated was detected by a sudden increase in acoustic emission and confirmed by microscopic examination.

The critical load and the corresponding coefficient of friction at the appearance of the first tensile crack can be determined around the scratch length of 114 μm, where the kinks or ripple structures occur in

Figure 10: SEM Images of scratch track for 2 μm TiAlN coated EN 353 steel substrate at different locations. (Start load- 10 N, Loading rate- 10 N/mm, Scratch speed- 1.0 mm/sec and Scratch stroke- 14 mm): (a) micrograph at 0.3 mm scratch length, (b) micrograph at 5.7 mm scratch length, and (c) micrograph at 9.1mm scratch length).

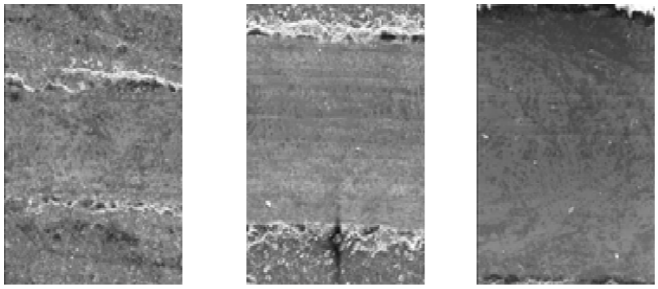

Figure 11: SEM images of scratch track for 2 μm AlCrN coated EN 353steel substrate at different locations. (Start load- 10 N, Loading rate- 10 N/mm, Scratch speed- 1.0 mm/sec and Scratch stroke- 14 mm: (a) micrograph at 0.3 mm scratch length, (b) micrograph at 4.9 mm scratch length, and (c) micrograph at 9.8 mm scratch length).

the vicinity marked by an arrow and become more remarkable as the scratch length or load increases for TiAlN coated samples. Both the critical load and the friction coefficient have been found to be 15.3N and 0.4, respectively.

It can be seen from Figure 7a that the cracks on the coating have been formed at the track without coating delamination. At higher applied loads a brittle failure mode of the coating was observed, as manifest by the formation of lateral cracks or chipping at the edges of the scratch tracks, as shown in Figure 10a. At this load, the driving force from the development of large tensile stresses at the edge of the scratch track is sufficiently high to cause the cracks to propagate across the TiAlN layer. One possible explanation for the formation of this kind of lateral crack is that the TiAlN microparticles act as stress raisers and cause the cracks to initiate. As the loading rate increases chipping at the edges of the scratch track and produces slight tensile cracks at load 60-70N, as shown in Figure 10b. This hypothesis is supported by the result of an event that is shown in Figure 10c. It is also evident that a through-thickness tensile crack travelled to the site of a macro-particle. Its propagation sheared the particle and produced the resulting circular lateral crack. The black coloration of the surface is due to the formation of oxides during wear testing.

SEM micrographs of the wear tracks of the AlCrN coated steel substrate are shown in Figures 11a-11c. It can be seen that this worn surface is characterized by scratches and plowing marks. The plowing action and particles pull-out as observed in Figure 11b are less severe for AlCrN coated steel substrate than the TiAlN coated steel substrate. The wear depth is also less for AlCrN coated steel substrate. Further, it was found that this failure mechanism was restricted to the coating, and no delamination from the substrate was observed for TiAlN coated steel substrate. Hence it can be inferred that EN-353 steel substrate has strong influence on both cohesive and adhesive strength of the TiAlN coating.

Conclusions

The TiAlN and AlCrN coatings were produced on EN-353 steel using cathodic arc evaporation method. The following conclusions can be drawn from our experimental investigations. Microstructure observations of coated steel substrates, few pores were detected optical micrographs. The thicker the deposition, the less porosity which could be due to substantial re-melting during the coating deposition. The AlCrN coating had a compound Vickers microhardness of Hv = 1094 which is higher than that of TiAlN coated samples. The compound hardness of both coatings increased with increase in coating thickness. The results of XRD data reveals that the grain size of TiAlN coating (15 nm) is less than that of AlCrN coating (21 nm). Sample TiAlN coating with thickness 2 μm showed a strong preferred lattice (ε) planes have a dominant orientation at 44.92° (2θ). The substrates coated with the AlCrN and TiAlN film, peaks protruding over the flat surface are quantitatively increased by the increase in coating thickness; the uniformity of the surface morphology can thus be improved. For the substrate with TiAlN and AlCrN coating, increase in coating thickness decreased the asperity. TiAlN coated steel substrate has higher surface roughness value and it seems that it is due to the variation in the particle size. With increase in the coating thickness, the amount of roughness also increased for TiAlN coated samples. Further, these samples showed higher wear loss and hence lower scratch resistance. The scratch resistance of AlCrN coated steel substrate was found to be superior to that of TiAlN coated samples. It could be attributed to be better adhesion of the AlCrN deposits in the steel substrate. Ploughing action and particles-pullout are the main wear mechanism of coatings.

References

1. Bautista Y, Gonzalez J, Gilabert J, Ibanez MJ, Sanz V (2011) Correlation between the wear resistance and the scratch resistance for nanocomposite coatings. Progress in Organic Coatings 70: 178-185.
2. Singer IL, Fayeulle S, Ehni PD (1996) Wear behaviour of triode-sputtered MoS_2 coatings in dry sliding contact with steel and ceramics. Wear 195: 7-20.
3. Low CTJ, Wills RGA, Walsh FC (2006) Electrodeposition of composite coatings containing nanoparticles in a metal deposit. Surface and Coating Technology 201: 371-383.
4. Gissler W, Jehn HA (1992) Advanced techniques for surface engineering. Springer Netherlands, Dordrecht, Netherlands.
5. Rickerby D, Matthews A (1991) Advanced surface coatings-A handbook for surface engineering. Springer Netherlands, Dordrecht, Netherlands.
6. Khlifi K, Cheikh Larbi AB (2014) Mechanical properties and adhesion of TiN monolayer and TiN/TiAlN nanolayer coatings. Journal of Adhesion Science and Technology 28: 85-96.
7. Totik Y (2010) Investigation of the adhesion of NbN coatings deposited by pulsed dc reactive magnetron sputtering using scratch tests. J Coat Technol Res 7: 485-492.
8. Lee YZ, Jeong KH (1998) Wear-life diagram of TiN-coated steels. Wear 217: 175-181.
9. Liu Y, Li L, Cai X, Chen Q, Xu M, et al. (2005) Effects of pretreatment by ion implantation and interlayer on adhesion between aluminum substrate and TiN film. Thin Solid Films 493: 152-159.
10. Su YL, Yao SH (1997) On the performance and application of CrN coating. Wear 205: 112-119.
11. Su YL, Yao SH, Leu ZL, Wei CS, Wu CT (1997) Comparison of tribological behaviour of three films-TiN, TiCN and CrN-grown by physical vapor deposition. Wear 213: 165-174.
12. Posti E, Nieminen I (1989) Influence of coating thickness on the life of TiN-coated high speed cutting tools. Wear 129: 273-283.
13. Guu YY, Lin JF (1996) Comparison of the tribological characteristics of titanium nitride and titanium carbonitride coating films. Surface and Coatings Technology 85: 146-155.
14. Fox-Rabinovich GS, Beake BD, Endrino JL, Veldhuis SC, Parkinson R, et al. (2006) Effect of mechanical properties measured at room and elevated temperatures on the wear resistance of cutting tools with TiAlN and AlCrN coatings. Surface & Coatings Technology 200: 5738-5742.
15. Chawla V, Chawla A, Mehta Y, Puri D, Prakash S, et al. (2011) Investigation of properties and corrosion behaviour of hard TiAlN and AlCrN PVD thin coatings in the 3 wt% NaCl solution. J Australian Ceramic Society 47: 48-55.
16. Aihua L, Jianxin D, Haibing C, Yangyang C, Jun Z (2012) Friction and wear properties of TiN, TiAlN, AlTiN and CrAlN PVD nitride coatings. Int J Refractory Metals & Hard Mat 31: 82-88.
17. Wang Y, Zhang P, Wu H, Wei D, Wei X, et al.(2014) Tribological properties of double-glow plasma surface niobizing on low-carbon steel. Tribology Transactions 57: 786-792.
18. Hedenqvist P, Olsson M, Jacobson S, Soderberg S (1990) Failure mode analysis of TiN-coated high speed steel: In situ scratch adhesion testing in the scanning electron microscope. Surface and Coatings Technology 41: 31-49.
19. Tushinsky L, IKovensky I, Plokhov A, Sindeyev V, Reshedko P (2002) Coated metal-structure and properties of metal-coating composites. Springer.
20. Xie Y, Hawthorne HM (2001) A model for compressive coating stresses in the scratch adhesion test. Surface and Coatings Technology 141: 15-25.
21. Nordin M, Larsson M (1999) Deposition and characterisation of multilayered PVD TiN/CrN coatings on cemented carbide. Surface and coatings technology 116: 108-115.
22. Nordin M, Larsson M (1999) Nano-galvanic coupling for enhanced Ag^+ release in ZrCN-Ag films: Antibacterial application. Surface and Coatings Technology 116:108-115.
23. Chawla V (2013) structural characterization and corrosion behavior of nanostructured TiAlN and AlCrN thin coatings in 3 wt% NaCl Solution. Journal of Materials Science and Engineering 3: 22-30.

24. Huanga LY, Xua KW, Lu J (2002) Evaluation of scratch resistance of diamond-like carbon films on Ti alloy substrate by nano-scratch technique. Diamond and Related Materials 11: 1505-1510.

25. Lee LH (1991) Fundamentals of adhesion. Springer Science, Business Media, LLC, New York.

26. Gissler W, Jehn HA (1992) Scratching of materials and applications. Kluwer Academic Publishers, Italy.

27. Takadoum J (1998) Materials and surface engineering in tribology. John Wiley & Sons Inc, USA.

28. Bunshah RF (2002) Handbook of hard coatings. William Andrew, USA.

29. Lacombe R (2005) Adhesion measurement methods: theory and practice. Taylor and Frances, CRC Press, New York.

30. Tracton AA (2005) Coatings technology handbook. CRC Press, USA.

31. Rickerby D, Matthews A (1991) Advanced surface coatings: A Handbook of surface engineering. Chapman & Hall, New York.

32. Tschiptschin AP, Garzon CM, Lopez DM (2006) The effect of nitrogen on the scratch resistance of austenitic stainless steels. Trib Inter 39: 167-174.

33. Seo TW, Weon JI (2012) Influence of weathering and substrate roughness on the interfacial adhesion of acrylic coating based on an increasing load scratch test. J Mater Sci 47: 2234-2240.

34. Savas S, Danisman S (2014) Multipass sliding wear behavior of TiAlN coatings using a spherical indenter: effect of coating parameters and duplex treatment. Tribology Transactions 57: 242-255.

35. Szameitat K (1992) Hard chrome technology Modern , in a line with Okonomie and ecology. pp: 124-136.